

Heavy-fermion behavior in a two-band Fermi liquid

Carlos Sanchez-Castro and Kevin S. Bedell

Los Alamos National Laboratory, T-11, MS B262 Los Alamos, New Mexico 87545

(Received 29 May 1992)

In this paper we present the calculation of the Landau parameters for a two-band Fermi liquid using the induced-interaction model. The model studied consists of two bands crossing the Fermi surface; one of these bands has electrons with a large crystalline mass and strong Coulomb correlations. The other band is made up of electrons with a small crystalline mass and negligible intraband correlations. For an antiferromagnetic coupling between the two bands, the system exhibits heavy-fermion behavior, i.e., very large linear in T -specific-heat coefficient, large T^2 term in the resistivity, and a small Wilson ratio. A ferromagnetic coupling between the two bands does not result in heavy-fermion behavior.

I. INTRODUCTION

In a recent paper Sanchez-Castro and Bedell¹ developed a generalization of the induced-interaction model²⁻⁷ to a two-component Fermi liquid. The one-component version of this model has been applied to a variety of systems. These include, among others, liquid ^3He ,^{2-4,7} strongly correlated electronic systems,^{3,4} and spin-polarized Fermi systems.^{5,6} It has been very successful in accounting for the properties of a variety of correlated Fermi systems, in particular unpolarized^{2-4,7} and polarized^{5,6} liquid ^3He . Some of the features of the heavy-fermion materials could also be accounted for within this model. However, it failed to account for one of the most prominent heavy-fermion signatures, the small value of the Wilson ratio, $R = \pi^2 k_B^2 \chi / 3\mu_B^2 \gamma$, where χ is the Pauli susceptibility and γ is the linear in T -specific-heat coefficient.

One of the approaches that has been extensively used in the heavy-fermion problem that gives a reasonable value for the Wilson ratio is the slave-boson approach⁸ to the Anderson lattice model.⁹ The suppression of the double occupancy of a single site by two f electrons is treated in the slave-boson mean field. This produces a renormalized band structure with large mass enhancements for the quasiparticles. If the interactions, which are of order $1/N_f$, with N_f the f -electron degeneracy, are ignored, then the Wilson ratio is equal to 1 with no room for deviations. The inclusion of interaction effects will give rise to small corrections, for large N_f , to the Wilson ratio.^{10,11} The interactions between the quasiparticles also lead to a superconducting instability.^{12,13} The pairing instability was predicted to be a d wave when terms of order $1/N_f$ were included.^{12,13} More recent calculations, including terms of order $(1/N_f)^2$, have opened up the possibility that a p wave is favored.¹⁴

A number of phenomenological models were proposed to account for the properties of heavy fermions. One of the more interesting was the single-component Fermi liquid of Pethick *et al.*¹⁵ used to study UPt_3 . This was interesting since it revealed that a single-component Fermi liquid could not provide a consistent account of UPt_3 . In particular, the large $T^3 \ln T$ term in the specific heat C_v

(Ref. 16) required that the Fermi-liquid parameter F_0^a was close to -0.8 , which gives a Wilson ratio close to 5. This discrepancy led Pethick and Pines¹⁷ to introduce a two-component phenomenology. At high temperature they¹⁷ begin with local moments and a conduction band which couple strongly at low temperature to yield a massive quasiparticle band. They argue that the magnetization is not conserved, due to strong spin-orbit interactions, and that this makes it difficult to relate the moment of the quasiparticles to the conduction electrons or the free-ion moments. This in principle could account for the discrepancy between the small Wilson ratio and the large $T^3 \ln T$ terms in the specific heat; however, no detailed calculations of the $T^3 \ln T$ terms within the Pethick and Pines¹⁷ model exist. Moreover, the extraction from experiment of the spin-nonconserving part of the magnetization is not straightforward, and estimates based on microscopic calculations do not exist. The evidence for abandoning some variation of a Fermi-liquid state, e.g., an anisotropic Fermi surface or a multiband scheme without spin orbit interactions, is not so clear.

While no detailed calculations exist for the $T^3 \ln T$ term of a single-component system with an anisotropic Fermi surface, we do not expect this to resolve the discrepancy between the small Wilson ratio and large $T^3 \ln T$ in some heavy-fermion systems. In such a Fermi liquid the various properties will involve averages of the quasiparticle velocity and interactions over the Fermi surface. To evaluate the Wilson ratio and the coefficient of the $T^3 \ln T$ term in C_v , very different averages are needed. Given the broad range of heavy-fermion materials, it would be hard to imagine that a realistic single-band picture could account for the systematics of these materials.

In the slave-boson treatment of the Anderson lattice model, the model of Pethick and Pines,¹⁷ and the single-component Fermi liquid model, there is only one heavy quasiparticle band at the Fermi level at low temperatures. While these models capture some of the many-body physics they miss the multiband character of the heavy-fermion materials. The multiband character is clearly evident in UPt_3 from the de Hass-van Alphen effect measurements of Taillefer *et al.*¹⁸ The structure of the Fermi surface obtained by Taillefer *et al.*¹⁸ is in remark-

ably good agreement with that predicted by several electronic band-structure calculations.¹⁸ The problem with the band-structure calculations¹⁹ is the effective-mass enhancement. The measured effective masses are from 10 to 25 times larger than the band masses.¹⁸ These large discrepancies suggest that the many-body correlations are significant; however, the underlying bandlike character of the quasiparticles is crucial.

To fully incorporate the band structure into a many-body calculation is beyond current technology. What we are proposing is a model that starts with a simplified band structure, a two-band model, with the many-body physics treated using the induced-interaction model developed by Sanchez-Castro and Bedell.¹ It is important to emphasize that our starting point is a band picture; we have no localized f electrons to begin with. The band structure we start with has electrons in one narrow band, with large band masses, and another broad band with much smaller masses. This simplified band picture is motivated in part by some work of Albers.²⁰ In this paper it is shown that an f -like band is formed when the platinum p electrons hybridize with the $5f$ electrons of the uranium. This is the narrow band at the Fermi level in our model, and our broad band is designed to model the $5d$ band of platinum. No additional effects of hybridization between the two bands are included. In principle, the effects of hybridization can be included in the induced-interaction equations; however, this is beyond the scope of the current calculation.

With the simplified starting model and the approximation introduced to obtain the induced-interaction equations,²⁻⁶ it is useful to explore the extent to which the essential many-body physics is preserved in the induced-interaction model. Direct checks on the approximations used to obtain the induced-interaction equations are not possible. However, some qualitative comparisons with other techniques can be made and some physical motivation can be used to understand the single-component model.

The structure of the induced interaction was originally motivated by Babu and Brown² using physical arguments. The approximations in which the frequency and momentum dependence of the quasiparticle interactions are ignored allows one to convert the multidimensional coupled nonlinear integral equations into one-dimensional coupled nonlinear integral equations. While these are drastic approximations they are constrained by the forward-scattering sum rule and the antisymmetrization of the scattering amplitude. More recently, there have been a number of calculations²¹⁻²³ that have tried to go beyond the approximations used in the induced-interaction approach. In particular, the work of Bickers and collaborators^{21,22} has included the third channel (the particle-particle channel) on an equal footing with the two particle-hole channels. Moreover, they have included the detailed energy and momentum dependence of their vertices.

The emphasis of Bickers and collaborators^{21,22} has been on the lattice system, and at present detailed comparisons with the induced-interaction approach are not possible. However, one of the approximations used by

Bickers and White²² is worth noting. The pseudopotential approximation introduced by Bickers and White²² is in the spirit of the induced-interaction approach. Here they use pseudopotentials obtained from the irreducible vertices evaluated at a particular value of the momentum and energy transfer. These are used to calculate the various dynamic susceptibilities which in turn are used to determine the effective interactions. The self-energy is then calculated and then fed back into the equations. This procedure is repeated until self-consistency is reached between the vertices and self-energies. This gives quite reasonable results for a number of properties.²² The main point to note here is the fact that the full energy and momentum dependence of the pseudopotentials is not needed to calculate some properties. The same approach has been used in the induced-interaction model. And while we have no comparable checks like those employed by Bickers and White,²² their results are most suggestive.

The work of Chen *et al.*²³ is also worth discussing at this point. In this work they study the magnetic properties of the two-dimensional Hubbard model using a modified RPA (random-phase approximation) to calculate the magnetic structure factor. The modifications involve replacing the Hubbard U by a renormalized interaction U_m . Here U_m arises in their work due to repeated scattering in the particle-particle channel. This effective interaction, in principle, is as well renormalized by repeated scattering in the exchange particle-hole channel, the induced interaction. Again, detailed comparisons between our approach and that of Chen *et al.*²³ are not possible; however, one of their qualitative conclusions is significant. They find that ferromagnetism is suppressed if you include the contributions from the other channel. This was found to be the case with the induced interaction model as well (see, for example, Ref. 4).

This paper is organized as follows: in Sec. II we describe the two-band system, whose many-body physics we propose to study using a Fermi-liquid formalism conveniently summarized in Sec. III. In Sec. IV, we restate the induced-interaction model for a two-component Fermi liquid recently introduced by the present authors. Next, in Sec. V, we develop an approximation for the direct interaction or driving term of the induced-interaction equations. Finally, in Sec. VI, we present the results of our calculation and a corresponding discussion. Section VII contains our concluding remarks.

II. THE TWO-BAND SYSTEM

We start by constructing a model Hamiltonian for the two-band system we propose to study. The Hamiltonian of a two-band system can be written quite generally as

$$H = H^0 + H' . \quad (2.1)$$

Here H^0 is the mean-field Hamiltonian obtained, for example, from an electronic structure calculation, and is given by

$$H^0 = \sum_{\mathbf{p}, i\sigma} t_{\mathbf{p}i}^0 a_{\mathbf{p}i\sigma}^\dagger a_{\mathbf{p}i\sigma} , \quad (2.2)$$

where $a_{\mathbf{p}i\sigma}^\dagger$ is a creation operator for an electron with crystal momentum \mathbf{p} , from band i and spin σ , and, $t_{\mathbf{p}i}^0$ is the corresponding band energy. H' is the residual interaction which can be written as

$$H' = H_{11} + H_{22} + H_{21}, \quad (2.3a)$$

$$H_{ii} = \frac{1}{2} \sum_{\substack{\mathbf{p}_1, \mathbf{p}_2, \mathbf{p}_3, \mathbf{p}_4 \\ \sigma_1, \sigma_2, \sigma_3, \sigma_4}} \langle \mathbf{p}_3 i \sigma_3; \mathbf{p}_4 i \sigma_4 | v | \mathbf{p}_1 i \sigma_1; \mathbf{p}_2 i \sigma_2 \rangle \\ \times a_{\mathbf{p}_3 i \sigma_3}^\dagger a_{\mathbf{p}_4 i \sigma_4}^\dagger a_{\mathbf{p}_2 i \sigma_2} a_{\mathbf{p}_1 i \sigma_1}, \quad (2.3b)$$

$$H_{21} = \sum_{\substack{\mathbf{p}_1, \mathbf{p}_2, \mathbf{p}_3, \mathbf{p}_4 \\ \sigma_1, \sigma_2, \sigma_3, \sigma_4}} (\langle \mathbf{p}_3 2 \sigma_3; \mathbf{p}_4 1 \sigma_4 | v | \mathbf{p}_1 2 \sigma_1; \mathbf{p}_2 1 \sigma_2 \rangle \\ - \langle \mathbf{p}_3 2 \sigma_3; \mathbf{p}_4 1 \sigma_4 | v | \mathbf{p}_2 1 \sigma_2; \mathbf{p}_1 2 \sigma_1 \rangle) \\ \times a_{\mathbf{p}_3 2 \sigma_3}^\dagger a_{\mathbf{p}_1 2 \sigma_1}^\dagger a_{\mathbf{p}_4 1 \sigma_4} a_{\mathbf{p}_2 1 \sigma_2}, \quad (2.3c)$$

where v is the two-body interaction.

Now, we specialize to a two-band system where both bands cross the Fermi surface. We assume that one of the two bands crossing the Fermi surface (say band 2) is very narrow and that the Coulomb correlations between electrons belonging to this band are large. The simplest choice of correlations between band-2 electrons is a repulsive, contact interaction (Stoner Hamiltonian) given by

$$H_{22} = U \sum_{\mathbf{p}, \mathbf{p}', \mathbf{q}} a_{\mathbf{p}+2\alpha}^\dagger a_{\mathbf{p}2\alpha} a_{\mathbf{p}'-2\beta}^\dagger a_{\mathbf{p}'2\beta}. \quad (2.4)$$

Here and throughout this work, we limit our consideration to normal or non-umklapp processes. In addition, we have taken the system volume $V=1$. The other band crossing the Fermi surface (band 1) is assumed to be a broad band with negligible intraband correlations. Therefore,

$$H_{11} = 0. \quad (2.5)$$

For the interaction between electrons belonging to different bands, we choose a contact, magnetic coupling of the form

$$H_{21} = -\frac{1}{2} \sum_{\substack{\mathbf{p}, \mathbf{p}', \mathbf{q} \\ \alpha, \beta, \alpha', \beta'}} J a_{\mathbf{p}+2\alpha}^\dagger \sigma_{\alpha\beta} a_{\mathbf{p}2\beta} a_{\mathbf{p}'-2\alpha'}^\dagger \sigma_{\alpha'\beta'} a_{\mathbf{p}'1\beta'}, \quad (2.6)$$

where σ is a vector whose components are the Pauli matrices. The parameter J is a constant chosen to be positive (negative) for ferromagnetic (antiferromagnetic) coupling. A term like this one usually appears in the two-band-system Hamiltonian even in the case of spin-independent residual interactions due to exchange. To see that, we note that for a contact, spin-independent interaction, we have

$$\langle \mathbf{p}+2\alpha; \mathbf{p}'-2\alpha' | v | \mathbf{p}'1\beta'; \mathbf{p}2\beta \rangle \\ = \frac{1}{2} \langle \mathbf{p}+2\alpha; \mathbf{p}'-2\alpha' | v | \mathbf{p}'1; \mathbf{p}2 \rangle (\delta_{\alpha\beta} \delta_{\alpha'\beta'} + \sigma_{\alpha\beta} \cdot \sigma_{\alpha'\beta'}). \quad (2.7)$$

Substituting this result into Eq. (2.3c) generates a magnetic coupling like in Eq. (2.6). Thus, in this case, the strength of the magnetic term coupling the electrons in the two bands is given by the band exchange matrix element.

To summarize, the two-band system we propose to study has initially a broad and a narrow band crossing the Fermi surface with Hamiltonian H^0 , given by Eq. (2.2), and a residual interaction H' given by Eqs. (2.3a), (2.4), (2.5), and (2.6), i.e., the total Hamiltonian of the system is

$$H = \sum_{\mathbf{p}, i, \sigma} t_{\mathbf{p}i}^0 a_{\mathbf{p}i\sigma}^\dagger a_{\mathbf{p}i\sigma} + U \sum_{\mathbf{p}, \mathbf{p}', \mathbf{q}} a_{\mathbf{p}+2\alpha}^\dagger a_{\mathbf{p}2\alpha} a_{\mathbf{p}'-2\beta}^\dagger a_{\mathbf{p}'2\beta} \\ - \frac{J}{2} \sum_{\substack{\mathbf{p}, \mathbf{p}', \mathbf{q} \\ \alpha, \beta, \alpha', \beta'}} a_{\mathbf{p}+2\alpha}^\dagger \sigma_{\alpha\beta} a_{\mathbf{p}2\beta} a_{\mathbf{p}'-2\alpha'}^\dagger \sigma_{\alpha'\beta'} a_{\mathbf{p}'1\beta'}. \quad (2.8)$$

This Hamiltonian is formally identical to the Kondo lattice Hamiltonian,²⁴ except for the form chosen for the band energies $t_{\mathbf{p}i}^0$. We will assume that both bands have a quadratic dispersion relation, and in the presence of interactions they become renormalized to

$$\epsilon_{\mathbf{p}i\sigma}^0 = \mu + \frac{1}{2m_i^*} (p^2 - p_F^{(i)2}), \quad (2.9)$$

where μ is the chemical potential, $p_F^{(i)} = \hbar k_F^{(i)}$, $k_F^{(i)} = (3\pi^2 n_i)^{1/3}$ is the Fermi wave vector and n_i is the particle density of the i th band, a fixed quantity in our calculation since we start with fully hybridized bands. Here m_i^* is the effective mass of the i th band, which, as we will discuss below in Sec. III, contains contributions from the crystal lattice and from electron-electron interactions. For the moment, we just state that the lattice contribution to the effective mass, called the crystalline mass m_i , is taken as a fixed parameter in our model. By setting the effective masses equal to the crystalline masses, the renormalized band energies Eq. (2.9) reduce to the band energies $t_{\mathbf{p}i}^0$ appearing in Eq. (2.2).

The phenomenological Hamiltonian describing this two-band system contains four parameters: the two crystalline masses m_i , the strength of the repulsion between the narrow band electrons U , and the strength of the interband magnetic coupling J . To study this strongly interacting Fermi liquid, we will calculate the quasiparticle interaction function using a generalization of the induced-interaction equations recently introduced by the authors and presented in Sec. IV. In the next section, for the sake of completeness, we will summarize some results of the Landau theory of a two-component Fermi liquid that are subsequently used to analyze our results.

III. LANDAU FERMI-LIQUID THEORY

In this work, we will study the many-body physics of the two-band system described in Sec. II through a Fermi-liquid formalism. This approach focuses on the calculation of the quasiparticle interaction function $f_{ij}^{\sigma\sigma'}(\mathbf{p}, \mathbf{p}')$, which describes how the quasiparticle energies are changed by their interactions with other quasiparticles by

$$\varepsilon_{\mathbf{p}i\sigma} = \varepsilon_{\mathbf{p}i\sigma}^0 + \sum_{\mathbf{p}'j\sigma'} f_{ij}^{\sigma\sigma'}(\mathbf{p}, \mathbf{p}') \delta n_{\mathbf{p}'j\sigma'} . \quad (3.1)$$

Here $\varepsilon_{\mathbf{p}i\sigma}^0$ is the equilibrium quasiparticle energy, $\delta n_{\mathbf{p}i\sigma} = n_{\mathbf{p}i\sigma} - n_{\mathbf{p}i\sigma}^0$ is the deviation in the distribution function $n_{\mathbf{p}i\sigma}$ from its equilibrium value $n_{\mathbf{p}i\sigma}^0$. A detailed discussion of the theory of a charged two-component Fermi liquid can be found in Ref. 1. In this section, we summarize some of the results which we subsequently use.

Fermi-liquid theory expresses the renormalization of the physical properties of a system of interacting fermions due to their mutual interactions in terms of Landau parameters. These are defined by the usual Legendre expansion of the quasiparticle interaction function

$$f_{ij}^{\sigma\sigma'}(\mathbf{p}, \mathbf{p}') = \sum_{l=0}^{\infty} f_{ij,l}^{\sigma\sigma'} P_l(\hat{\mathbf{p}} \cdot \hat{\mathbf{p}}') . \quad (3.2)$$

Some frequently occurring combinations of Landau parameters are

$$f_{ij}^s(\mathbf{p}, \mathbf{p}') = \frac{1}{2} [f_{ij}^{\uparrow\uparrow}(\mathbf{p}, \mathbf{p}') + f_{ij}^{\downarrow\downarrow}(\mathbf{p}, \mathbf{p}')] , \quad (3.3a)$$

$$f_{ij}^a(\mathbf{p}, \mathbf{p}') = \frac{1}{2} [f_{ij}^{\uparrow\downarrow}(\mathbf{p}, \mathbf{p}') - f_{ij}^{\downarrow\uparrow}(\mathbf{p}, \mathbf{p}')] . \quad (3.3b)$$

The static properties of the system we are interested in are the specific heat at constant volume C_V , the magnetic susceptibility χ , and the Wilson ration R , defined by

$$R = \frac{\pi^2 k_B^2}{3\mu_B^2} \frac{\chi}{\gamma(0)} , \quad (3.4)$$

where $\gamma(0)$ is the linear in T -specific-heat coefficient, and μ_B is the Bohr magneton.

The specific heat at a constant volume and fixed number of electrons in each band (N_1, N_2) is given by^{1,25}

$$C_V = T \left[\frac{\partial s}{\partial T} \right]_{V, N_1, N_2} = \gamma(0) T , \quad (3.5)$$

where s is the entropy density, $\gamma(0) = (\pi^2/3)k_B^2 [N_1(0) + N_2(0)]$, and $N_i(0) = m_i^* p_F^{(i)} / (\pi^2 \hbar^3)$ is the density of states of the i th band crossing the Fermi surface. Here m_i^* is the effective mass of the i th component at the Fermi surface.

The magnetic susceptibility can be obtained from the induced magnetization m divided by the magnitude of the external magnetic field, H , and for small values of H is given by^{1,26}

$$\chi = \frac{m}{H} = \sum_{i=1}^2 N_i(0) \mu_B^2 a_i , \quad (3.6)$$

where

$$a_i = \frac{1 + f_{jj,l=0}^a N_j(0) - f_{ij,l=0}^a N_j(0)}{D^a(0)}$$

and

$$D^a(0) = [1 + f_{11,l=0}^a N_1(0)] [1 + f_{22,l=0}^a N_2(0)] - (f_{21,l=0}^a)^2 N_1(0) N_2(0) .$$

Here we have assumed that spin-nonconserving interac-

tions (such as the spin-orbit coupling) are negligible and to a good approximation the magnetic moment of the i th band electron equals μ_B . As stressed in Ref. 1, both the numerator and denominator of the magnetic susceptibility must be separately positive to guarantee the stability of the Fermi-liquid state. This requirement does not preclude, however, that one of the terms in Eq. (3.6), i.e., a partial susceptibility, be negative as long as the total sum be positive. Thus, the formula for the magnetic susceptibility of a two-component system is considerably richer than for a one-component Fermi liquid.

For a two-band system with spherical Fermi surface branches, such as ours, the effective masses, the crystalline masses, and the $l=1$ spin-symmetric Landau parameters are related by¹

$$\frac{m_i^*}{m_i} = \frac{1}{1 - \frac{1}{3} N_i^0(0) \left[f_{ii,l=1}^s + \left(\frac{p_F^{(j)}}{p_F^{(i)}} \right)^2 \frac{m_j}{m_i} f_{ij,l=1}^s \right]} \quad (i \neq j) , \quad (3.7)$$

where

$$N_i^0(0) = \frac{p_F^{(i)} m_i}{\pi^2 \hbar^3} .$$

This relation, which is formally equivalent to the expression obtained for a Gallilan invariant system provided one replaces the crystalline masses by the bare mass, is a consequence of the isotropy of the system. The crystalline masses give the effective-mass enhancements due to the periodic potential of the ions; the $l=1$ spin-symmetric Landau parameters give the additional enhancements due to the electron-electron interactions. As stressed in Ref. 27, the potential used in most band calculations is taken to be that of the bare ions screened by the electron response. Thus, the decomposition presented here is not always feasible, and the effective-mass enhancements obtained from a band calculation do not always correspond to the crystalline masses appearing in Eq. (3.7).

Once the quasiparticle interaction is determined, we are interested in calculating the resistivity and studying pairing correlations in the model. To calculate them, we must first obtain an expression for the quasiparticle scattering amplitude in terms of the quasiparticle interaction function. There are several ways to derive this relation. One route starts from the Bethe-Salpeter equation for the four-point function, while the other approach begins from the Landau kinetic equation.²⁸ The final result of both approaches is

$$A_{ij}^{s(a)}(\mathbf{k}, \mathbf{k}') = \sum_{l=0}^{\infty} A_{ij,l}^{s(a)} P_l(\hat{\mathbf{k}} \cdot \hat{\mathbf{k}}') \quad (3.8a)$$

and

$$B_{ij}^{s(a)}(\mathbf{k}, \mathbf{k}') = \sum_{l=0}^{\infty} B_{ij,l}^{s(a)} P_l(\hat{\mathbf{k}} \cdot \hat{\mathbf{k}}') . \quad (3.8b)$$

Here $A_{ij}^{s(a)}, B_{ij}^{s(a)}$ are the spin-symmetric (antisymmetric) scattering amplitude and band-flip scattering amplitude¹

at finite exchange momentum transfer $q = \hbar|\mathbf{k} - \mathbf{k}'|$ expressed in a series of Legendre polynomials in terms of the angle between \mathbf{k} and \mathbf{k}' . For $l=0,1$, it has been shown that^{1,5}

$$A_{ii,l}^{s(a)} = \frac{f_{ii,l}^{s(a)}(1 - f_{jj,l}^{s(a)}X_{jj}^l) + (f_{ij,l}^{s(a)})^2 X_{jj}^l}{D_l^{s(a)}} \quad (i \neq j), \quad (3.9a)$$

$$A_{21,l}^{s(a)} = \frac{f_{21,l}^{s(a)}}{D_l^{s(a)}}, \quad (3.9b)$$

$$B_l^{s(a)} = \frac{g_l^{s(a)}}{1 - g_l^{s(a)}X_{21}^l}, \quad (3.9c)$$

where

$$D_l^{s(a)} = (1 - f_{22,l}^{s(a)}X_{22}^l)(1 - f_{11,l}^{s(a)}X_{11}^l) - (f_{21,l}^{s(a)})^2 X_{22}^l X_{11}^l,$$

$$X_{ij}^l(\mathbf{q}) = 2 \int \frac{d^3\mathbf{p}'}{(2\pi\hbar)^3} \frac{n_{\mathbf{p}'+\mathbf{q},i} - n_{\mathbf{p}',j}}{\varepsilon_{\mathbf{p}'+\mathbf{q},i} - \varepsilon_{\mathbf{p}',j}} \left[\frac{1 - \hat{\mathbf{q}} \cdot \hat{\mathbf{p}}'^2}{2} \right]^l,$$

and $n_{\mathbf{p}_i} = \theta(p_F^{(i)} - p)$. Here θ is a step function and explicit expressions for the $X_{ij} \equiv X_{ij}^{l=0}$ are given in Sec. IV.

Except for some accurate transport calculations,⁷ Eqs. (3.8) and (3.9) are not normally used; instead, a simpler approximation due to Dy and Pethick,²⁹ the s - p approximation, is often introduced. To perform this approximation, we must first express the scattering amplitudes in terms of the Abrikosov and Khalatnikov angles (θ, ϕ) , the angle between the incoming momenta, and the angle between the incoming and outgoing scattering planes, respectively. The s - p approximation in the one-component case expresses $A^{\sigma\sigma'}(\theta, \phi)$ as a linear polynomial in $\cos\phi$, the coefficient determined from certain restrictions. First, we must require that the forward-scattering amplitudes $A^{\sigma\sigma'}(\theta, \phi=0)$ agree with the expansion in terms of Landau parameters truncated after the $l=1$ term. In addition, we must require, under the interchange of outgoing quasiparticle momenta ($\phi \rightarrow \phi + \pi$), that the triplet (singlet) scattering amplitude be antisymmetric (symmetric).

To generalize the s - p approximation to the two-band system, we again expand the scattering amplitudes in a linear polynomial in $\cos\phi$. The coefficients are chosen such that the forward-scattering amplitudes are matched and the resulting scattering amplitude has the right behavior under exchange ($\phi \rightarrow \phi + \pi$). For the intraband scattering amplitude, the derivation is identical to the one-component case and gives

$$A_{ii}^{\uparrow\uparrow}(\theta, \phi) = \sum_{l=0}^1 (A_{ii,l}^s + A_{ii,l}^a) \cos\phi P_l(\cos\theta), \quad (3.10a)$$

$$A_{ii}^{\uparrow\downarrow}(\theta, \phi) = \frac{1}{2} \sum_{l=0}^1 [(A_{ii,l}^s - 3A_{ii,l}^a) + (A_{ii,l}^s + A_{ii,l}^a) \cos\phi] P_l(\cos\theta). \quad (3.10b)$$

For the interband scattering amplitude, it is shown in the Appendix that the approximation gives

$$A_{21}^{\uparrow\uparrow}(\theta, \phi) = \frac{1}{2} \sum_{l=0}^1 [(A_{21,l}^s + A_{21,l}^a - B_l^s - B_l^a) + (A_{21,l}^s + A_{21,l}^a + B_l^s + B_l^a) \cos\phi] \times P_l(\cos\theta), \quad (3.11a)$$

$$A_{21}^{\uparrow\downarrow}(\theta, \phi) = \frac{1}{2} \sum_{l=0}^1 [(A_{21,l}^s - A_{21,l}^a - 2B_l^a) + (A_{21,l}^s - A_{21,l}^a + 2B_l^a) \cos\phi] \times P_l(\cos\theta), \quad (3.11b)$$

$$B^{\uparrow\uparrow}(\theta, \phi) = -A_{21}^{\uparrow\uparrow}(\theta, \phi + \pi), \quad (3.11c)$$

$$B^{\uparrow\downarrow}(\theta, \phi) = -[A_{21}^{\uparrow\uparrow}(\theta, \phi + \pi) - A_{21}^{\uparrow\downarrow}(\theta, \phi + \pi)]. \quad (3.11d)$$

The calculation of the resistivity, ρ , proceeds as described in Ref. 1. There, the non-umklapp contribution to the resistivity is calculated from

$$\frac{1}{\rho} = \frac{1}{3} e^2 \sum_{i,j,k=1}^2 \left[[N_i(0)\tau_i(0)N_k(0)\tau_k(0)]^{1/2} v_i S_{ij} \times \sum_{\nu \text{ odd}} \frac{2\nu + 1}{\nu(\nu + 1)[\nu(\nu + 1) - 2\lambda_j]} S_{jk}^T v_k \right], \quad (3.12)$$

where S_{ij} is a 2×2 matrix (S_{ij}^T being its transpose) that diagonalizes λ_{ij} , a 2×2 matrix involving angular averages of the scattering amplitude. The λ_j are the eigenvalues of this matrix, i.e.,

$$\sum_{j,l} S_{ij}^T \lambda_{jl} S_{lk} = \lambda_i \delta_{ik}. \quad (3.13)$$

Here $v_i, \tau_i(0)$ are, respectively, the Fermi velocity and the quasiparticle lifetime of the i th band electrons at the Fermi surface, and e is the electron charge.

To construct the matrix λ_{ij} for a two-band electron system, we first define the transition probabilities

$$W_{ii} = \frac{1}{2} W_{i\uparrow, i\uparrow} + W_{i\uparrow, i\downarrow} \quad (3.14a)$$

and

$$W_{ij} = W_{i\uparrow, j\uparrow} + W_{i\uparrow, j\downarrow} + W_{(i\uparrow, j\downarrow; i\downarrow, j\uparrow)} \quad (i \neq j), \quad (3.14b)$$

where

$$W_{i\sigma, j\sigma'} = \frac{2\pi}{\hbar} |A_{ij}^{\sigma\sigma'}(\theta, \phi)|^2$$

and

$$W_{(i\uparrow, j\downarrow; i\downarrow, j\uparrow)} = \frac{2\pi}{\hbar} |B^{\uparrow\downarrow}(\theta, \phi + \pi)|^2.$$

Then the matrix λ_{ij} is given for ($p_F^{(i)} = p_F^{(j)}$) by

$$\lambda_{ii} = \left[\int \frac{d\Omega}{4\pi} \frac{W_{ii}}{2 \cos(\theta/2)} (-\hat{\mathbf{p}}_1 \cdot \hat{\mathbf{p}}_2 + \hat{\mathbf{p}}_1 \cdot \hat{\mathbf{p}}_3 + \hat{\mathbf{p}}_1 \cdot \hat{\mathbf{p}}_4) \right. \\ \left. + \left(\frac{m_j^*}{m_i^*} \right)^2 \int \frac{d\Omega}{4\pi} \frac{W_{ij}}{2 \cos(\theta/2)} \hat{\mathbf{p}}_1 \cdot \hat{\mathbf{p}}_3 \right] / W_i \\ (i \neq j) \quad (3.15a)$$

and

$$\lambda_{ij} = \int \frac{d\Omega}{4\pi} \frac{W_{ij}}{2 \cos(\theta/2)} (-\hat{\mathbf{p}}_1 \cdot \hat{\mathbf{p}}_2 + \hat{\mathbf{p}}_1 \cdot \hat{\mathbf{p}}_4) / (W_i W_j)^{1/2} \\ (i \neq j), \quad (3.15b)$$

where $d\Omega = \sin\theta d\theta d\phi$,

$$W_i = \int \frac{d\Omega}{4\pi} \frac{W_{ii}}{2 \cos(\theta/2)} + \left(\frac{m_j^*}{m_i^*} \right)^2 \int \frac{d\Omega}{4\pi} \frac{W_{ij}}{2 \cos(\theta/2)} \\ (i \neq j),$$

$$\hat{\mathbf{p}}_1 \cdot \hat{\mathbf{p}}_2 = \cos\theta,$$

$$\hat{\mathbf{p}}_1 \cdot \hat{\mathbf{p}}_3 = 1 - \frac{1}{2}(1 - \cos\theta)(1 - \cos\phi),$$

and

$$\hat{\mathbf{p}}_1 \cdot \hat{\mathbf{p}}_4 = 1 - \frac{1}{2}(1 - \cos\theta)(1 + \cos\phi).$$

In terms of these transition probabilities, the quasiparticle lifetimes are given by

$$\frac{1}{\tau_i(0)} = \frac{m_i^{*3} (k_B T)^2}{16\pi^2 \hbar^6} W_i. \quad (3.16)$$

As discussed in Ref. 1, we neglect the eigenvalue of λ_{ij} equal to 1, which is an artifact of neglecting umklapp or momentum-nonconserving processes in the calculation of ρ . Thus, by keeping only the other eigenvalue of λ_{ij} , we are assuming that the interband scattering is much larger than the intraband scattering between electrons. The effectiveness of the umklapp scattering depends in detail on the band structure and the Fermi surface. For simple metals with nearly spherical Fermi surfaces, the effectiveness of the umklapp scattering is small;³⁰ however, for tight-binding bands it is most efficient.^{30,31} In either case, the intraband scattering will be smaller than or at most comparable to the interband scattering. Thus, the calculation for the interband scattering in the two-band model should give a reasonable estimate of the resistivity.

Another quantity we can readily calculate in our model is the intraband pairing interaction for L -wave pairing. According to the Patton-Zarighalam formula,³² the critical temperature due to L -wave intraband pairing of the i th band is given by

$$T_{c,ii}^L = 1.13 a_i T_F^{(i)} e^{1/g_{ii}^L}, \quad (3.17)$$

where a_i is a constant independent of the density and in general different for each band, $T_F^{(i)} = p_F^{(i)2} / (2m_i^* k_B)$, and g_{ii}^L is the i th band intraband pairing interaction for L -wave pairing. The intraband pairing interaction for sing-

let ($L=0$) and triplet ($L=1$) pairing is given by (keeping up to $l=1$ partial waves)

$$g_{ii}^{L=0} = \frac{1}{4} N_i(0) \sum_{l=0}^1 (-1)^l (A_{ii,l}^s - 3A_{ii,l}^a), \quad (3.18)$$

$$g_{ii}^{L=1} = \frac{1}{12} N_i(0) \sum_{l=0}^1 (-1)^l (A_{ii,l}^s + A_{ii,l}^a) \\ = \frac{1}{6} N_i(0) (A_{ii,l=0}^s + A_{ii,l=0}^a). \quad (3.19)$$

Here we have made use of the forward-scattering sum rule¹

$$\sum_{l=0}^1 (A_{ii,l}^s + A_{ii,l}^a) = 0.$$

IV. CALCULATION OF THE QUASIPARTICLE INTERACTION FUNCTION: THE INDUCED INTERACTION MODEL

To calculate the quasiparticle interaction function, we will use the induced-interaction equations for a two-component Fermi liquid obtained by Sanchez-Castro and Bedell.¹ These are coupled, integral equations for the quasiparticle interaction and antisymmetrized scattering amplitudes on the Fermi surface. They allow us to think of the Landau f function as divided into a direct part d and an induced part f_{ind} ,

$$f(\mathbf{p}, \mathbf{p}') = d(\mathbf{p}, \mathbf{p}') + f_{\text{ind}}(\mathbf{p}, \mathbf{p}'). \quad (4.1)$$

The induced interaction is the contribution to the quasiparticle interaction due to its coupling to the collective modes of the system, i.e., the contribution due to multiple propagation and scattering of a particle-hole pair. The induced term has the same form for all Fermi systems. The direct term, however, contains the details about the specific system considered and must be calculated from the bare Hamiltonian. Once calculated, the direct term acts as a driving term in the integral equations. In the case where the particles in the system have a short-range interaction, the direct interaction would have a predominantly short-range nature, and the induced interactions, mediated by virtual collective excitations, would have long-range contributions. The structure of the induced interaction guarantees that any antisymmetric approximation for the direct interaction yields an antisymmetric scattering amplitude. Thus, as stressed by Quader,³³ this approach is an approximation to the full parquet series for the quasiparticle interactions (see Fig. 1).

The induced-interaction equations for an unpolarized, two-compound Fermi liquid are¹

$$f_{22}^2(\mathbf{p}, \mathbf{p}') = d_{22}^s - \frac{1}{2} \frac{(f_{22}^s)^2 X_{22} (1 - f_{11}^s X_{11})}{D^s} \\ - \frac{1}{2} \frac{(f_{21}^s)^2 X_{11} (1 + f_{22}^s X_{22})}{D^s} \\ - \frac{3}{2} \frac{(f_{22}^a)^2 X_{22} (1 - f_{11}^a X_{11})}{D^a} \\ - \frac{3}{2} \frac{(f_{21}^a)^2 X_{11} (1 + f_{22}^a X_{22})}{D^a}, \quad (4.2a)$$

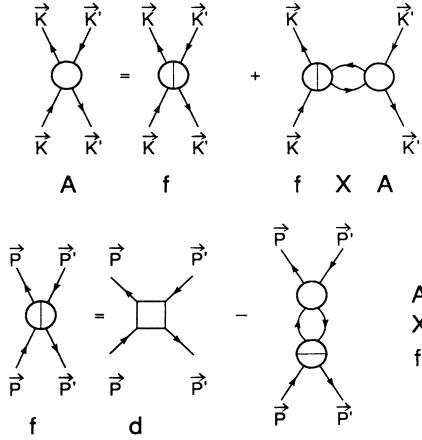


FIG. 1. Schematic representation of the induced interaction equations.

$$f_{11}^s(\mathbf{p}, \mathbf{p}') = d_{11}^s - \frac{1}{2} \frac{(f_{11}^s)^2 X_{11} (1 - f_{22}^s X_{22})}{D^s} - \frac{1}{2} \frac{(f_{21}^s)^2 X_{22} (1 + f_{11}^s X_{11})}{D^s} - \frac{3}{2} \frac{(f_{11}^a)^2 X_{11} (1 - f_{22}^a X_{22})}{D^a} - \frac{3}{2} \frac{(f_{21}^a)^2 X_{22} (1 + f_{11}^a X_{11})}{D^a}, \quad (4.2b)$$

$$f_{22}^a(\mathbf{p}, \mathbf{p}') = d_{22}^a - \frac{1}{2} \frac{(f_{22}^s)^2 X_{22} (1 - f_{11}^s X_{11})}{D^s} - \frac{1}{2} \frac{(f_{21}^s)^2 X_{11} (1 + f_{22}^s X_{22})}{D^s} + \frac{1}{2} \frac{(f_{22}^a)^2 X_{22} (1 - f_{11}^a X_{11})}{D^a} + \frac{1}{2} \frac{(f_{21}^a)^2 X_{11} (1 + f_{22}^a X_{22})}{D^a}, \quad (4.2c)$$

$$f_{11}^a(\mathbf{p}, \mathbf{p}') = d_{11}^a - \frac{1}{2} \frac{(f_{11}^s)^2 X_{11} (1 - f_{22}^s X_{22})}{D^s} - \frac{1}{2} \frac{(f_{21}^s)^2 X_{22} (1 + f_{11}^s X_{11})}{D^s} + \frac{1}{2} \frac{(f_{11}^a)^2 X_{11} (1 - f_{22}^a X_{22})}{D^a} + \frac{1}{2} \frac{(f_{21}^a)^2 X_{22} (1 + f_{11}^a X_{11})}{D^a}, \quad (4.2d)$$

$$f_{21}^s(\mathbf{p}, \mathbf{p}') = d_{21}^s - \frac{1}{2} \frac{(g^s)^2 X_{21}}{1 - g^s X_{21}} - \frac{3}{2} \frac{(g^a)^2 X_{21}}{1 - g^a X_{21}}, \quad (4.2e)$$

$$f_{21}^a(\mathbf{p}, \mathbf{p}') = d_{21}^a - \frac{1}{2} \frac{(g^s)^2 X_{21}}{1 - g^s X_{21}} + \frac{1}{2} \frac{(g^a)^2 X_{21}}{1 - g^a X_{21}}, \quad (4.2f)$$

$$g^s(\mathbf{p}, \mathbf{p}') = {}_1d^s - \frac{1}{2} \frac{f_{21}^s X_{11} f_{11}^s (1 - f_{22}^s X_{22})}{D^s} - \frac{1}{2} \frac{f_{21}^s X_{22} [f_{22}^s + (f_{21}^s)^2 X_{11}]}{D^s} - \frac{3}{2} \frac{f_{21}^a X_{11} f_{11}^a (1 - f_{22}^a X_{22})}{D^a} - \frac{3}{2} \frac{f_{21}^a X_{22} [f_{22}^a + (f_{21}^a)^2 X_{11}]}{D^a}, \quad (4.2g)$$

and

$$g^a(\mathbf{p}, \mathbf{p}') = {}_1d^a - \frac{1}{2} \frac{f_{21}^s X_{11} f_{11}^s (1 - f_{22}^s X_{22})}{D^s} - \frac{1}{2} \frac{f_{21}^s X_{22} [f_{22}^s + (f_{21}^s)^2 X_{11}]}{D^s} + \frac{1}{2} \frac{f_{21}^a X_{11} f_{11}^a (1 - f_{22}^a X_{22})}{D^a} + \frac{1}{2} \frac{f_{21}^a X_{22} [f_{22}^a + (f_{21}^a)^2 X_{11}]}{D^a}, \quad (4.2h)$$

where

$$D^{s(a)} = (1 - f_{22}^{s(a)} X_{22})(1 - f_{11}^{s(a)} X_{11}) - (f_{21}^{s(a)})^2 X_{22} X_{11}.$$

Here we have written the full quasiparticle interaction as $f_{ij}^{s(a)}(\mathbf{p}, \mathbf{p}')$ and kept only the contribution to the induced interaction due to the $l=0$ Landau moments, $f_{ij}^{s(a)} \equiv f_{ij, l=0}^{s(a)}$. The function $X_{ij}(\mathbf{q}')$ was calculated in Ref. 5 for a quasiparticle dispersion relation $\varepsilon_{\mathbf{p}i\sigma} = \mu + (p^2 - p_F^{(i)2}) / (2m_i^*)$, where μ is the chemical potential, and is given by

$$X_{ii}(\mathbf{q}') = -\frac{1}{2} N_i(0) \left[1 + \left[\frac{q'}{4p_F^{(i)}} - \frac{p_F^{(i)}}{q'} \right] \ln \left| \frac{p_F^{(i)} - q'/2}{p_F^{(i)} + q'/2} \right| \right]$$

and

$$X_{21}(\mathbf{q}') = \frac{-1}{2\pi^2 \hbar^3} M \left[p_F^{(2)} - p_F^{(1)} - \frac{1}{4} \left[y \frac{m_2^* + m_1^*}{m_2^* - m_1^*} - \frac{p_F^{(2)2} - p_F^{(1)2}}{y} \right] \ln \left| \frac{1+A}{1-A} \right| + \frac{1}{2} M \mu \ln \left| \frac{1+B}{1-B} \right| \right],$$

where

$$y = (p_F^{(2)2} + p_F^{(1)2} - 2p_F^{(1)}p_F^{(2)} \cos\theta)^{1/2},$$

$$M = \frac{m_1^* m_2^*}{m_2^* - m_1^*},$$

$$A = \frac{(p_F^{(1)} + p_F^{(2)})y}{y^2 + p_F^{(1)}p_F^{(2)}(1 + \cos\theta)},$$

$$B = \frac{u \left[\frac{p_F^{(2)}}{m_2^*} + \frac{p_F^{(1)}}{m_1^*} \right]}{u^2 + \frac{p_F^{(1)}p_F^{(2)}}{m_1^* m_2^*} (1 + \cos\theta)},$$

and

$$u = \left[\left[\frac{p_F^{(2)}}{m_2^*} \right]^2 + \left[\frac{p_F^{(1)}}{m_1^*} \right]^2 - 2 \left[\frac{p_F^{(1)}}{m_1^*} \right] \left[\frac{p_F^{(2)}}{m_2^*} \right] \cos\theta \right]^{1/2}.$$

One interpretation of these equations is as follows: the induced-interaction term for f_{22}^s , for example, contains four distinct contributions. The first (third) is an induced interaction between two component-2 quasiparticles by interchanging a density (spin-density) fluctuation of its own component. Those terms are also present, in the induced interaction for a one-component Fermi liquid² but with different screening factors. The second (fourth) contribution is an induced interaction of two component-2 quasiparticles mediated by the interchange of a density (spin-density) fluctuation in component 1. This effect is analogous to the Ruderman-Kittel-Kasuya-Yusida (RKKY) magnetic interaction between distant localized spins mediated by an interaction with an itinerant electron gas.³⁴ In our case, however, both components are itinerant. The RKKY interaction is calculated using second-order perturbation theory; our theory, however, takes into account further screening effects that go beyond second-order perturbation theory.

One important feature of these equations is that they are symmetrical, i.e., by interchanging component labels in Eq. (4.2a), we obtain Eq. (4.2b), the quasiparticle interaction between two component-1 quasiparticles. Thus, we have a “reverse RKKY” effect in which the interaction between two component-1 quasiparticles is also mediated by interchanging a fluctuation in the other component. Since the interaction between quasiparticles in each component is affected by the coupling to the other component, we must solve these coupled equations simultaneously in order to be able to account for all feedback effects.

It should be noted that although we have retained only up to $l=0$ moments in the induced interactions, Eqs. (4.2), in principle, any number of moments can be projected out from the full particle-hole interaction. This is a consequence of introducing the \mathbf{q}' dependence through the phase-space functions $X_{ij}(\mathbf{q}')$. Even the projected $l=0$ moments on the left will be coupled to the $l=1$ moments, in addition to the $l=0$ moments on the right. This is because the phase-space functions $X_{ij}(\mathbf{q}')$ are dependent on the $l=1$ moment of the quasiparticle in-

teraction through the m_i^* . Thus, any numerical solution of these equations must be performed in a self-consistent way.

V. DIRECT INTERACTION

To calculate the direct interaction, we must sum all particle-hole irreducible diagrams. In this work, we will approximate it by keeping only the diagrams linear in U and J . These diagrams themselves constitute the Hartree-Fock approximation to the quasiparticle interaction function.¹ Since all pair interactions are contact interactions, the direct interaction has only an $l=0$ moment and is given by

$$d_{i_1 i_3; i_2 i_4}^{\sigma_1 \sigma_3; \sigma_2 \sigma_4}(\mathbf{p}, \mathbf{p}') = \langle \mathbf{p} i_3 \sigma_3; \mathbf{p}' i_4 \sigma_4 | H' | \mathbf{p} i_1 \sigma_1; \mathbf{p}' i_2 \sigma_2 \rangle. \quad (5.1)$$

Substituting the residual interaction Hamiltonian Eq. (2.3) into the above expression and making use of the definitions,

$$d_{ij}^{s(a)} = \frac{1}{2} (d_{ii; jj}^{\uparrow \uparrow; \uparrow \uparrow} \pm d_{ii; jj}^{\uparrow \downarrow; \downarrow \downarrow}), \quad (5.2a)$$

$${}_1 d^{s(a)} = \frac{1}{2} (d_{21; 12}^{\uparrow \uparrow; \uparrow \uparrow} \pm d_{21; 12}^{\uparrow \downarrow; \downarrow \downarrow}). \quad (5.2b)$$

We readily get for the direct interactions

$$d_{11}^{s(a)} = 0, \quad d_{22}^{s(a)} = \pm U/2, \quad d_{21}^s = 0, \quad d_{21}^a = -J/2, \quad (5.3)$$

$${}_1 d^s = \frac{3}{4}J, \quad \text{and} \quad {}_1 d^a = -\frac{J}{4}.$$

Equations (5.3) are the driving terms used in solving the induced-interaction equations. The approximation that sets the quasiparticle interaction equal to the Hartree-Fock approximation yields results for the response functions entirely equivalent to the random-phase approximation.^{1,27} Thus, the induced interactions for this case represent the effect of correlations that go beyond the random-phase approximation.

VI. RESULTS AND DISCUSSION

The two-band system studied has four adjustable parameters, namely U , J , and the two crystalline masses. For the cases we study with $U \gg J$ the results depend on only three parameters J , m_1 , and m_2 . The solutions for the induced-interaction equations, Eq. (4.2), for certain choices of the adjustable parameters are shown in Tables I–III and in Figs. 2–6. All calculations were done assuming an equal number of electrons in each of the two bands, $n_1 = n_2 = n$ and a fixed value of $nU = 11.18$ eV, where U is the matrix element of the band-2–band-2 interaction Hamiltonian, namely Eq. (2.4). The crystalline mass of the “light” electrons (band 1) was set equal to five times the bare electron mass, m_e , while the crystalline mass for the heavy electrons (band 2) was varied between $5m_e$ and $50m_e$. Calculations were performed for positive (negative) nJ , i.e., ferromagnetic (antiferromagnetic) interband coupling. The most interesting of our results given in Table II is that for $m_2/m_e = 50$ and negative nJ , the two-band system displays heavy-fermion behavior in

TABLE I. Landau parameters as a function of nJ (eV), m_1, m_2 . We assumed equal number of electrons in each band, i.e., $k_F^{(1)} = k_F^{(2)} = k_F = 1/\text{\AA}$ and fixed $nU = 11.18$ eV. Both the direct interactions and the Landau parameters are presented in a dimensionless way by multiplying by $5m_e p_F / (\pi^2 \hbar^3)$. Here m_e is the electron mass. The values used for the crystalline masses are denoted by m_i .

nJ	m_2/m_e	m_1/m_e	f_{22}^s	f_{11}^s	f_{21}^s	b_{21}^s	f_{22}^a	f_{11}^a	f_{21}^a	b_{21}^a
3.05	5.0	5.0	22.75	0.52	2.86	6.32	-0.35	0.07	-0.33	-0.27
1.52	5.0	5.0	22.68	0.31	1.37	3.34	-0.39	-0.02	-0.27	-0.23
0	5.0	5.0	22.51	0.00	0.00	0.00	-0.50	0.00	0.00	0.00
-1.52	5.0	5.0	24.91	3.16	3.50	-0.40	0.58	0.72	1.06	2.46
-3.05	5.0	5.0	27.13	5.44	5.84	-0.38	1.35	1.48	1.80	4.01
3.05	50.0	5.0	22.10	0.65	2.94	6.13	-0.03	0.08	-0.12	-0.09
1.52	50.0	5.0	22.09	0.49	1.45	3.15	-0.03	-0.02	-0.10	-0.08
0	50.0	5.0	22.06	0.00	0.00	0.00	-0.05	0.00	0.00	0.00
-1.52	50.0	5.0	23.51	6.76	1.87	-0.10	0.46	2.07	1.07	1.28
-3.05	50.0	5.0	25.43	14.72	2.46	-0.10	1.10	4.73	2.37	1.67

TABLE II. Various physical properties as a function of nJ (eV), m_1, m_2 for the system described in Table I. The linear term in the specific heat $\gamma(0)$, the magnetic susceptibility X , and the T^2 term in the resistivity α are expressed in $\text{mJ}/(\text{cm}^3 \text{K}^2)$, $10^{-3} \text{emu}/\text{cm}^3$, and $\mu\Omega \text{cm}/\text{K}^2$, respectively.

nJ	m_2/m_e	m_1/m_e	X	$\gamma(0)$	R	α	m_2^*/m_e	m_1^*/m_e
3.05	5.0	5.0	0.028	0.65	3.16	8.22×10^{-4}	6.87	5.69
1.52	5.0	5.0	0.026	0.64	3.01	4.31×10^{-4}	6.70	5.52
0	5.0	5.0	0.015	0.58	1.88	0.00	6.16	5.00
-1.52	5.0	5.0	0.003	1.11	0.22	5.15	10.92	10.46
-3.05	5.0	5.0	0.002	1.21	0.12	28.6	11.80	11.52
3.05	50.0	5.0	0.195	3.93	3.62	4.04×10^{-3}	68.82	6.75
1.52	50.0	5.0	0.190	3.89	3.56	3.47×10^{-3}	68.13	6.59
0	50.0	5.0	0.124	3.52	2.57	0.00	62.63	5.00
-1.52	50.0	5.0	0.098	6.38	1.12	1.74	99.93	22.72
-3.05	50.0	5.0	0.096	6.54	1.08	2.18	101.66	23.90

TABLE III. The magnetic moments and the intraband pairing interaction as a function of nJ (eV), m_1, m_2 for the system described in Table I. The magnetic moments in each band are denoted by a_i , i.e., $X = \sum_i N_i(0) \mu_B^2 a_i$. In this model, we found no intraband singlet pairing in either band. The intraband triplet pairing interaction is denoted by $g_{ii}^{L=1} = [N_i(0)/6] A_{ii, i=0}^{\uparrow\uparrow}$.

nJ	m_2/m_e	m_1/m_e	a_2	a_1	$g_{22}^{L=1}$	$g_{11}^{L=1}$
3.05	5.0	5.0	3.72	2.49	-0.13	-0.03
1.52	5.0	5.0	3.56	2.34	-0.13	-0.02
0	5.0	5.0	2.60	1.00	-0.11	0.00
-1.52	5.0	5.0	0.48	-0.05	-0.35	-0.31
-3.05	5.0	5.0	0.28	-0.04	-0.40	-0.38
3.05	50.0	5.0	3.39	5.91	-0.16	-0.05
1.52	50.0	5.0	3.34	5.83	-0.16	-0.05
0	50.0	5.0	2.69	1.0	-0.12	0.00
-1.52	50.0	5.0	2.54	-5.13	-0.46	-0.45
-3.05	50.0	5.0	2.54	-5.15	-0.48	-0.48

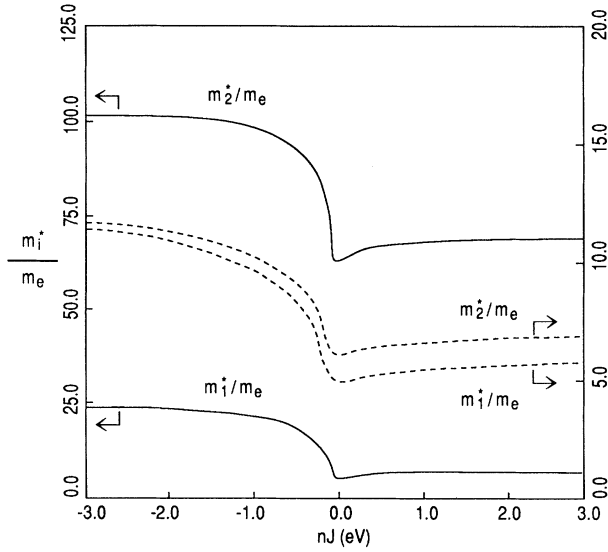


FIG. 2. Ratio of the effective mass to the bare electron mass for the system described in Table I. Here and throughout Figs. 2–6, the solid curve stands for the results obtained when taking the crystalline masses $m_2/m_e=50.0$ and $m_1/m_e=5.0$ and the dotted curve stands for the case when $m_2/m_e=m_1/m_e=5.0$.

the sense of an enhanced linear in T term in the specific heat, a quenched magnetic susceptibility, which leads to a Wilson ratio of the order of 1. To understand the physics of these results, we must consider now a more detailed analysis.

To start with, we first consider the effective-mass enhancements as they appear in Table II and Fig. 2. It is clear from Table II that an antiferromagnetic interband coupling is more effective in generating mass enhancements in both bands than a ferromagnetic coupling. As

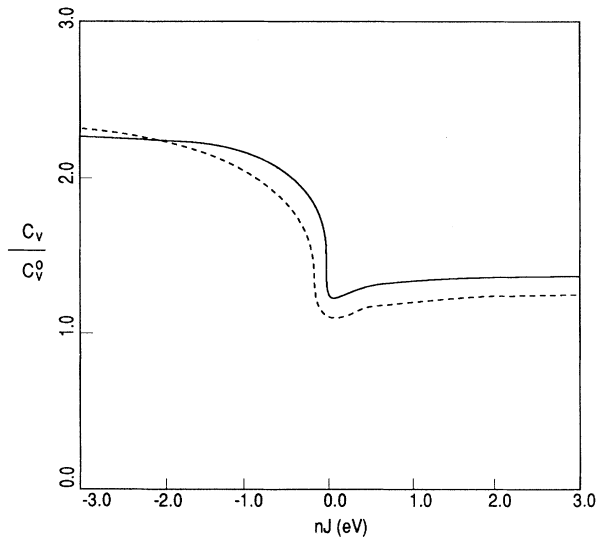


FIG. 3. The ratio of the heat capacity, C_v , to the band heat capacity, $C_v^0 = \gamma^0(0)T$. Here $\gamma^0(0) = (\pi^2/3)k_B^2 \sum_i N_i^0(0)$. We have $\gamma^0(0) = 2.86 \text{ mJ}/(\text{K}^2 \text{ cm}^3)$ for the solid curve and $\gamma^0(0) = 0.52 \text{ mJ}/(\text{K}^2 \text{ cm}^3)$ for the dotted curve.

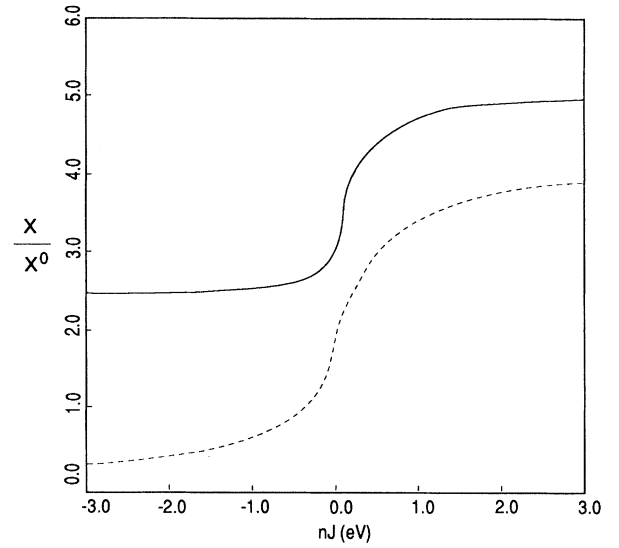


FIG. 4. The ratio of the magnetic susceptibility, χ , to the band magnetic susceptibility $\chi^0 = \mu_B^2 \sum_i N_i^0(0)$. Here $\chi^0 = 0.039 \times 10^{-3} \text{ emu}/\text{cm}^3$ for the solid curve and $\chi^0 = 0.007 \times 10^{-3} \text{ emu}/\text{cm}^3$ for the dotted curve.

we will later elaborate in the discussion of the resistivity, the antiferromagnetic coupling gives a strong interband scattering rate, which results in a rapid frequency dependence of the self-energy and large effective masses.³⁵ Another feature of these results is that for large nJ , the mass enhancements seem to saturate, a result we will later discuss in more detail in reference to the magnetic susceptibility. In addition, it should be noted that the percentage increase in the effective mass of the light electrons is much larger than the one for the heavy electrons (band 2). To understand this trend, we must consider the term $(p_F^{(j)}/p_F^{(i)})^2 (m_j/m_i) f_{ij,l=1}^s$ ($i \neq j$) that appears in the denominator of the effective-mass equation, Eq. (3.7). This term corresponds physically to the contribution of

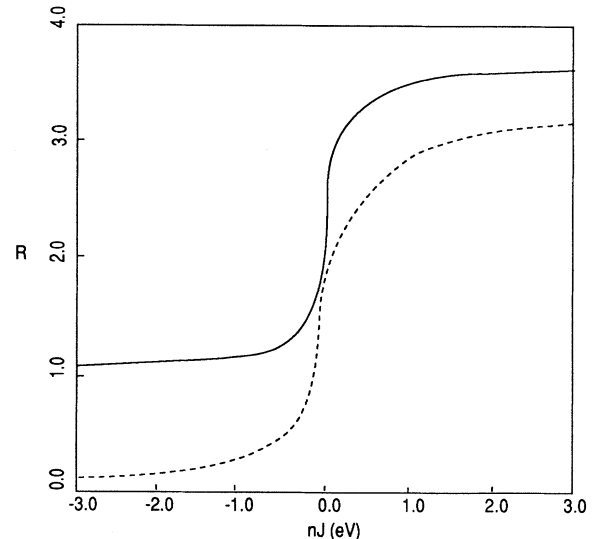


FIG. 5. The Wilson ratio.

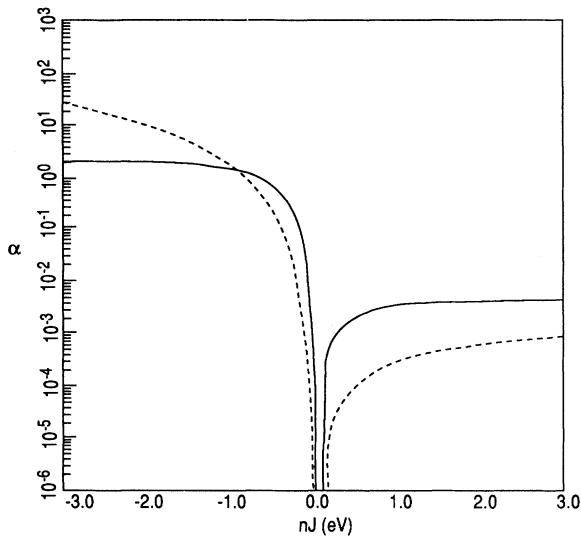


FIG. 6. Semilogarithmic graph of the T^2 term of the resistivity, α , expressed in $\mu\Omega \text{ cm}/\text{K}^2$.

the i th effective mass due to the backflow of the other component. Clearly, for very different crystalline masses, the renormalization of the light electron mass as they propagate must be larger since they must displace the much more massive electrons of the other component, and vice versa. Thus, in effect, as we crank up nJ , both types of electrons become heavy. To summarize, the linear in T term in the specific heat, being essentially the sum of the density of states of the two bands at the Fermi surface, is greatly enhanced for antiferromagnetic coupling in comparison with ferromagnetic coupling (see Fig. 3).

Now, we consider the most interesting of our results, the behavior of the magnetic susceptibility. The results shown in Table II and Fig. 4 give a magnetic susceptibility which is decreased (enhanced) over its $nJ=0$ limit for antiferromagnetic (ferromagnetic) coupling. To understand this effect, it is crucial to consider the expression for the magnetic susceptibility, Eq. (3.6), and the sign of $f_{21,l=0}^a$. We can interpret Eq. (3.6) as the sum of the partial susceptibilities of each of the two bands. Clearly, as discussed in Sec. III, one of the partial susceptibilities can be negative as long as their sum is positive as required for the stability of the Fermi liquid. In addition, from Table I, it is evident that for antiferromagnetic coupling f_{21}^a is positive since that coupling lowers the energy of a pair of band-2–band-1 electrons with opposite spins compared to the similar spin arrangement. Thus, as Table III shows, for antiferromagnetic coupling the magnetization of the “light band” points in the opposite direction to the one of the “heavy band” and they tend to cancel. This cancellation of the partial magnetizations is analogous to the Kondo screening of a local moment by the conduction electrons, except that in our case the “local-moment” band is not flat but somewhat delocalized for large m_2/m_e . For the case of ferromagnetic coupling, both magnetizations point in the same direction and add to an enhanced total magnetic susceptibility. We stress

the fact that for large m_2/m_e the partial susceptibilities in both bands are well enhanced over their $nJ=0$ limit for both couplings. This is easily seen from Tables II and III by noting that the partial susceptibilities are proportional to the product $m_i^* a_i$, which is equal to 1 for an ideal Fermi gas.

The physical picture that we can draw from these results is the following: the large repulsive U induces ferromagnetic correlations in the heavy band. A magnetic coupling of any sign will induce these ferromagnetic correlations in the light band. The enhanced partial susceptibilities are a consequence of this effect. The sign of nJ determines the relative alignment of the magnetizations.

It is evident from this analysis why the physics seems to saturate with nJ ; i.e., once the partial susceptibilities lock relative to each other, further increases in nJ have an insignificant effect. The quenched susceptibility and enhanced linear in T term in the specific heat give a Wilson ratio R given by Eq. (3.4) and shown in Table II and Fig. 5, which for $m_2/m_e=50$ is of the order of 1 for antiferromagnetic interband coupling. In contrast, for ferromagnetic coupling $R \approx 3$, due to the enhanced magnetic susceptibility and not so dramatic increase in $\gamma(0)$.

This picture brings about the interesting possibility that an antiferromagnetically coupled two-band Fermi liquid could display metamagnetism, in the sense first introduced by Wohlfarth and Rhodes,³⁶ in the presence of a large external magnetic $\mu_B B_{\text{ext}} > nJ$ which breaks the internal locking of the partial magnetizations. In addition to a real metamagnetic transition, a “near”-metamagnetic transition, as proposed by Bedell and Sanchez-Castro³⁷ for liquid ^3He , is possible. This in fact is a more realistic possibility within our model, and experiments here could provide a clear test of our band-based picture versus the local-moment picture provided by the Anderson lattice. It has been argued by Stamp³⁸ that the application of a large magnetic field would cause an unbinding of the local moment and the conduction electron in the Anderson lattice. At high fields there would remain a light conduction band and a lattice of weakly interacting local moments. In our picture, the resulting state would consist of two bands with much smaller masses, since the interband spin fluctuations would be suppressed. As a function of temperature, we expect the thermal fluctuations to increase as the temperature is increased and these will tend to suppress the antialignment of the band magnetizations. This in turn will decrease the masses and result in two bands that are close in mass to the $J=0$ starting bands. The important point to emphasize is that at high fields or high temperatures we will have two bands present, which is distinct from the Anderson lattice model or the Pethick ad Pines model.¹⁷

Support for a band picture can be found in photoemission experiments. Photoemission experiments have been carried out as a function of temperature on UPt_3 and UBe_{13} .³⁹ The main conclusion is that at low T there is a narrow band at the Fermi level and at high T there is little change.^{39,40} At first sight, the picture that we have of a narrow band and a broad one at high temperatures appears inconsistent with the thermodynamic properties of

the heavy fermions. In particular, the Curie or Curie-Weiss behavior of χ for large T is suggestive of local moments. It should be noted, however, that for $T \gg T_F$ a Fermi liquid also has a Curie-like susceptibility. For UPt₃ a single-band picture would give a T_F of the order of 100 K and so by room temperature we could have $\chi \sim 1/T$. That this behavior is possible in a strongly correlated system can be seen in liquid ³He. In ³He at $T \gtrsim T_F$, the spin susceptibility is of the Curie form.⁴¹ This is at a temperature far less than one might have expected. We do not wish to argue that the high-temperature behavior of heavy-fermion materials is just that of nondegenerate narrow-band electrons. However, we wish to point out that this is not incompatible with the observed behavior in these heavy-fermion systems.

In Table III, we also show values for the intraband triplet interaction. That the triplet interaction is attractive and singlet pairing is not predicted (repulsive) is very plausible within the framework of enhanced ferromagnetic correlations within each band for any nonzero nJ . The critical temperature of the system defined by the highest T_c predicted cannot be determined since we do not calculate the constants a_i appearing in the Patton-Zarringhalam formula, Eq. (3.17).

In Table II and Fig. 6, we also present the results of a calculation of the non-umklapp part of the resistivity due to electron-electron scattering as outlined in Sec. III. The calculation was done using an s approximation for the scattering amplitudes. It is evident from these results that for a fixed m_2/m , an antiferromagnetic coupling gives a larger T^2 term in the resistivity than a ferromagnetic one. This property, as well as the large effective-mass enhancements for antiferromagnetic coupling, are due to an enhanced scattering rate and a rapid energy dependence of the electron self-energy.³⁵ The conductivity is proportional to the imaginary part of the self-energy while the effective mass is proportional to the real part, thus large mass enhancements are consistent with large T^2 terms in the resistivity.

VII. CONCLUSIONS

In conclusion, the residual interactions in the two-band Fermi liquid just described with antiferromagnetic interband coupling induce ferromagnetic correlations in each band and lock the partial magnetizations against each other. This correlated state has an enhanced linear in T term in the specific heat, a quenched magnetic susceptibility, a small Wilson ratio, and a large T^2 term in the resistivity: all signatures of heavy-fermion behavior. The properties of the system saturate with increasing J . A strong external magnetic field that aligns the magnetizations of the two bands will produce a state with masses closer to the zero interband coupling limit.

ACKNOWLEDGMENTS

C.S.C. acknowledge partial support from Grants Nos. U.S. DOE DE-FG02-88ER40388 (Stony Brook) and U.S. DOE DE-FG05-89 ER45386 (West Virginia).

APPENDIX: THE s - p APPROXIMATION

In this appendix, we will show how to make an s - p approximation for the scattering amplitudes. These scattering amplitudes could be used in the calculation of transport processes and the study of pairing mechanisms between quasiparticles. As usual, the scattering amplitudes are described by the Abrikosov and Khalatnikov angles (θ, ϕ) , the angle between the incoming momenta \mathbf{p}_1 and \mathbf{p}_2 , and the angle between the plane defined by the incoming momenta \mathbf{p}_1 and \mathbf{p}_2 and the plane defined by the outgoing momenta \mathbf{p}_3 and \mathbf{p}_4 , respectively. We will assume that we know the forward-scattering amplitudes, i.e.,

$$A_{ij}^{s(a)}(\theta, \phi=0) = \sum_{l=0}^1 A_{ij,l}^{s(a)} P_l(\cos\theta) \quad (\text{A1})$$

and

$$B^{s(a)}(\theta, \phi=0) = \sum_{l=0}^1 B_l^{s(a)} P_l(\cos\theta). \quad (\text{A2})$$

The $A_{ij}^{s(a)}$ and $B_l^{s(a)}$, for example, can be obtained from Eq. (3.11) evaluated with $q=0$ in X_{11} , X_{22} , and $q=p_F^{(2)}-p_F^{(1)}$ in X_{21} . The construction of the s - p approximation for the $A_{ii}^{s(a)}(\theta, \phi)$ is very similar to the one-component case,²⁹ and we will merely state the result,

$$A_{ii}^{\uparrow\uparrow}(\theta, \phi) = \sum_{l=0}^1 (A_{ii,l}^s + A_{ii,l}^a) \cos\phi P_l(\cos\theta) \quad (\text{A3})$$

and

$$A_{ii}^{\uparrow\downarrow}(\theta, \phi) = \frac{1}{2} \sum_{l=0}^1 [(A_{ii,l}^s - 3A_{ii,l}^a) + (A_{ii,l}^s + A_{ii,l}^a) \cos\phi] P_l(\cos\theta). \quad (\text{A4})$$

For $A_{21}^{\uparrow\uparrow}(\theta, \phi)$, we must be more careful. We know that under exchange of \mathbf{p}_3 and \mathbf{p}_4 ($\phi \rightarrow \phi + \pi$),

$$A_{21}^{\uparrow\uparrow}(\theta, \phi + \pi) = -B^{\uparrow\uparrow}(\theta, \phi) \quad (\text{A5a})$$

or

$$B^{\uparrow\uparrow}(\theta, \phi + \pi) = -A_{21}^{\uparrow\uparrow}(\theta, \phi). \quad (\text{A5b})$$

In addition, Eqs. (A1) and (A2) give

$$A_{21}^{\uparrow\uparrow}(\theta, \phi=0) = \sum_{l=0}^1 (A_{21,l}^s + A_{21,l}^a) P_l(\cos\theta) \quad (\text{A6})$$

and

$$B^{\uparrow\uparrow}(\theta, \phi=0) = \sum_{l=0}^1 (B_l^s + B_l^a) P_l(\cos\theta). \quad (\text{A7})$$

To solve for the $A_{21}^{\uparrow\uparrow}(\theta, \phi)$ and $B^{\uparrow\uparrow}(\theta, \phi)$, we write

$$A_{21}^{\uparrow\uparrow}(\theta, \phi) = \sum_{l=0}^1 (a_l + \beta_l \cos\phi) P_l(\cos\theta) \quad (\text{A8})$$

and

$$B^{\uparrow\uparrow}(\theta, \phi) = \sum_{l=0}^1 (\gamma_l + \delta_l \cos\phi) P_l(\cos\theta). \quad (\text{A9})$$

Using Eq. (A5) with $\phi=0$ and Eqs. (A6) and (A7), we can determine $a_l, \beta_l, \gamma_l, \delta_l$. We obtain

$$A_{21}^{\uparrow\uparrow}(\theta, \phi) = \frac{1}{2} \sum_{l=0}^1 [(A_{21,l}^s + A_{21,l}^a - B_l^s - B_l^a) + (A_{21,l}^s + A_{21,l}^a + B_l^s + B_l^a) \cos\phi] \times P_l(\cos\theta) \quad (\text{A10})$$

and

$$B^{\uparrow\uparrow}(\theta, \phi) = \frac{1}{2} \sum_{l=0}^1 [(B_l^s + B_l^a - A_{21,l}^s - A_{21,l}^a) + (B_l^s + B_l^a + A_{21,l}^s + A_{21,l}^a) \cos\phi] \times P_l(\cos\theta). \quad (\text{A11})$$

A similar procedure is done with $A_{21}^{\downarrow\downarrow}(\theta, \phi)$. We know that under exchange of \mathbf{p}_3 and \mathbf{p}_4 ,

$$A_{21}^{\downarrow\downarrow}(\theta, \phi + \pi) = -2B^a(\theta, \phi) \quad (\text{A12a})$$

or

$$B^a(\theta, \phi + \pi) = -\frac{1}{2} A_{21}^{\downarrow\downarrow}(\theta, \phi). \quad (\text{A12b})$$

In addition, Eqs. (A1) and (A2) give

$$A_{21}^{\uparrow\downarrow}(\theta, \phi=0) = \sum_{l=0}^1 (A_{21,l}^s - A_{21,l}^a) P_l(\cos\theta) \quad (\text{A13})$$

and

$$B^a(\theta, \phi=0) = \sum_{l=0}^1 B_l^a P_l(\cos\theta). \quad (\text{A14})$$

Solving these equations in an analogous way to Eqs. (A8) and (A9), we obtain

$$A_{21}^{\uparrow\downarrow}(\theta, \phi) = \frac{1}{2} \sum_{l=0}^1 [(A_{21,l}^s - A_{21,l}^a - 2B_l^a) + (A_{21,l}^s - A_{21,l}^a + 2B_l^a) \cos\phi] P_l(\cos\theta) \quad (\text{A15})$$

and

$$B^a(\theta, \phi) = \frac{1}{2} \sum_{l=0}^1 \{ [B_l^a - \frac{1}{2}(A_{21,l}^s - A_{21,l}^a)] + [B_l^a + \frac{1}{2}(A_{21,l}^s - A_{21,l}^a)] \cos\phi \} P_l(\cos\theta). \quad (\text{A16})$$

$B^{\uparrow\downarrow}(\theta, \phi)$ follows from

$$B^{\uparrow\downarrow}(\theta, \phi) = B^{\uparrow\uparrow}(\theta, \phi) - 2B^a(\theta, \phi). \quad (\text{A17})$$

Thus, we have the desired generalization of the s - p approximation to a two-component Fermi liquid.

- ¹C. Sanchez-Castro and K. S. Bedell, Phys. Rev. B **43**, 12 874 (1991).
²S. Babu and G. E. Brown, Ann. Phys. (N.Y.) **78**, 1 (1973).
³T. L. Ainsworth, K. S. Bedell, G. E. Brown, and K. F. Quader, J. Low Temp. Phys. **50**, 319 (1983).
⁴K. S. Bedell and K. F. Quader, Phys. Rev. B **32**, 3296 (1985); K. F. Quader, K. S. Bedell, and G. E. Brown, *ibid.* **36**, 156 (1987).
⁵K. F. Quader and K. S. Bedell, J. Low Temp. Phys. **58**, 89 (1985).
⁶C. Sanchez-Castro and K. S. Bedell, J. Low Temp. Phys. **75**, 95 (1989).
⁷T. L. Ainsworth and K. S. Bedell, Phys. Rev. B **35**, 8425 (1987).
⁸P. Coleman, Phys. Rev. B **29**, 3035 (1984).
⁹A. Yoshimori and H. Kasin, J. Magn. Magn. Mater. **31**, 475 (1983).
¹⁰A. J. Millis and P. A. Lee, Phys. Rev. B **35**, 3394 (1987).
¹¹P. A. Lee, T. M. Rice, J. W. Serene, L. J. Sham, and J. W. Wilkins, Comments Condens. Matter Phys. **12**, 99 (1986), and references therein.
¹²A. Auerbach and K. Levin, Phys. Rev. Lett. **57**, 877 (1986).
¹³M. Lavagna, A. J. Millis, and P. A. Lee, Phys. Rev. Lett. **58**, 266 (1987).
¹⁴A. Houghton, N. Read, and H. Won, Phys. Rev. B **37**, 3782 (1988).
¹⁵C. J. Pethick, D. Pines, K. F. Quader, K. S. Bedell, and G. E. Brown, Phys. Rev. Lett. **57**, 1955 (1986).
¹⁶G. R. Stewart, Z. Fisk, J. O. Willis, and J. L. Smith, Phys. Rev. Lett. **52**, 679 (1984). For an extensive study of $T^3 \ln T$ effects in UPt₃ see A. De Visser, Ph.D. thesis, University of Amsterdam, 1989, and references therein.
¹⁷C. J. Pethick and D. Pines, in *Proceedings of the International*

- Workshop on Novel Mechanisms of Superconductivity*, edited by S. A. Wolf and V. Z. Kresin (Plenum, New York, 1987), pp. 201–214.
¹⁸L. Taillefer and G. G. Lonzarich, Phys. Rev. Lett. **60**, 1570 (1988); L. Taillefer, R. Newbury, G. G. Lonzarich, Z. Fisk, and J. L. Smith, J. Magn. Magn. Mater. **63&64**, 372 (1987).
¹⁹C. S. Wang, M. R. Norman, R. C. Albers, A. M. Boring, W. E. Pickett, H. Krakauer, and N. E. Christensen, Phys. Rev. B **35**, 7260 (1987); T. Oguchi, A. J. Freeman, and G. W. Crabtree, J. Magn. Magn. Mater. **63&64**, 645 (1987); R. C. Albers, A. M. Boring, and N. E. Christensen, Phys. Rev. B **33**, 8116 (1986).
²⁰R. C. Albers, Phys. Rev. B **32**, 7646 (1985).
²¹N. E. Bickers and D. J. Scalapino, Ann. Phys. (N.Y.) **193**, 206 (1989).
²²N. E. Bickers and S. R. White, Phys. Rev. B **43**, 8044 (1991).
²³L. Chen, C. Bourbonnais, T. Li, and A.-M. S. Tremblay, Phys. Rev. Lett. **66**, 369 (1991).
²⁴P. Coleman, Phys. Rev. B **28**, 5255 (1983).
²⁵J. Oliva and N. W. Ashcroft, Phys. Rev. B **23**, 6399 (1981).
²⁶I. A. Akhiezer and E. M. Chudnovskii, Zh. Eksp. Teor. Fiz. **66**, 2303 (1974) [Sov. Phys. JETP **39**, 1135 (1974)].
²⁷D. Pines and P. Nozières, *The Theory of Quantum Liquids* (Benjamin, New York, 1966), Vol. I.
²⁸C. Sanchez-Castro, K. S. Bedell, and S. A. J. Wieggers, Phys. Rev. B **40**, 437 (1989).
²⁹K. Dy and C. Pethick, Phys. Rev. **185**, 373 (1969).
³⁰W. E. Lawrence and J. W. Wilkins, Phys. Rev. B **7**, 2317 (1973).
³¹L. N. Bulaevskii, Adv. Phys. **37**, 443 (1988).
³²B. Patton and A. Zaringhaleh, Phys. Lett. **55A**, 95 (1975).
³³K. F. Quader, in *Windsurfing the Fermi Sea*, edited by T. T.

- Kuo and J. Speth (Elsevier, New York, 1987), Vol. 2, p. 390.
- ³⁴M. A. Ruderman and C. Kittel, *Phys. Rev.* **96**, 99 (1954).
- ³⁵G. E. Brown, C. J. Pethick, and A. Zaringhalam, *J. Low Temp. Phys.* **48**, 349 (1982).
- ³⁶E. P. Wohlfarth and P. Rhodes, *Philos. Mag.* **7**, 1817 (1962).
- ³⁷K. S. Bedell and C. Sanchez-Castro, *Phys. Rev. Lett.* **57**, 854 (1986).
- ³⁸P. C. E. Stamp, *Phys. Rev. Lett.* **59**, 517 (1987).
- ³⁹A. J. Arko, C. G. Olson, D. M. Wieliczka, Z. Fisk, and J. L. Smith, *Phys. Rev. Lett.* **53**, 2050 (1984).
- ⁴⁰A. J. Arko (private communication).
- ⁴¹B. T. Beal and J. Hatton, *Phys. Rev.* **139**, 1751 (1965).